

Role of nucleon-nucleon correlation in transport coefficients and gravitational-wave-driven r -mode instability of neutron stars

X. L. Shang,^{1,2} P. Wang,³ W. Zuo,^{1,2} and J. M. Dong^{1,2,*}

¹*Institute of Modern Physics, Chinese Academy of Sciences, Lanzhou 730000, China*

²*School of Physics, University of Chinese Academy of Sciences, Beijing 100049, China*

³*National Astronomical Observatories, Chinese Academy of Sciences, Beijing 100012, China*

(Dated: March 19, 2022)

The thermal conductivity and shear viscosity of dense nuclear matter, along with the corresponding shear viscosity timescale of canonical neutron stars (NSs), are investigated, where the effect of Fermi surface depletion (i.e., the Z-factor effect) induced by the nucleon-nucleon correlation are taken into account. The factors which are responsible for the transport coefficients, including the equation of state for building the stellar structure, nucleon effective masses, in-medium cross sections, and the Z-factor at Fermi surfaces, are all calculated in the framework of the Brueckner theory. The Fermi surface depletion is found to enhance the transport coefficients by several times at high densities, which is more favorable to damping the gravitational-wave-driven r -mode instability of NSs. Yet, the onset of the Z-factor-quenched neutron triplet superfluidity provides the opposite effects, which can be much more significant than the above mentioned Z-factor effect itself. Therefore, different from the previous understanding, the nucleon shear viscosity is still smaller than the lepton one in the superfluid NS matter at low temperatures. Accordingly, the shear viscosity cannot stabilize canonical NSs against r -mode oscillations even at quite low core temperatures 10^6 K.

As a class of compact objects, neutron stars (NSs) with typical mass $M \sim 1.4M_\odot$ and radii $R \sim 10$ km, contain extreme neutron-rich matter at supranuclear density in their interiors. Interestingly, they have many extreme features that cannot be produced in terrestrial laboratories, such as extremely strong magnetic field, superstrong gravitational field, extremely high density, superfluid matter and superprecise spin period [1], suggesting their importance for fundamental physics. These intriguing features have drawn great interest for researchers of various branches of contemporary physics and astronomy since the discovery of pulsars (rapidly rotating NSs) in 1967.

Due to the dense matter with large isospin asymmetry inside NSs, a great deal of attention has been paid to the recent astronomical observations that can be used to uncover the knowledge of the NS interior. For instance, the observations of stellar cooling enables one to constrain the equation of state (EOS) of dense matter, superfluidity and transport properties, in combination with indispensable theoretical analysis [2–8]. Moreover, a rapidly rotating NS is regarded as a gravitational wave source due to r -mode instability. The r -mode is a non-radial oscillation mode with Coriolis force as restoring force, which leads to the gravitational wave radiation in rapidly rotating NSs due to the Chandrasekhar-Friedmann-Schutz instability [9–11] and thus prevents the NSs from reaching their Kepler rotational frequency [12, 13]. The gravitational radiation is in turn able to excite r modes in NS core and hence enhances their oscillation amplitudes, and it is particularly interesting from the perspective of the gravitational wave observations with ground-based facilities. The gravitational wave signal from the r -mode oscillation, if detectable in the future, could help one to probe the dense matter properties inside NSs.

The reliable knowledge about transport coefficients of dense matter is crucial for understanding the stellar thermal evolution and r -mode-instability induced gravitational radiation. The thermal conductivity which measures the ability to conduct the heat, is an important input for modeling NS cooling [14, 15]. The shear viscosity is the primary damping mechanism that hinders the gravitational-wave-driven r -mode instability of rapidly rotating NSs at low temperatures ($< 10^9$ K) [16–18]. These two transport coefficients have been calculated by several authors based on the formalism derived by Abrikosov and Khalatnikov (AK) from the Landau kinetic equations for a multicomponent systems [19], where the required in-medium nucleon-nucleon cross sections is obtained by employing the correlated basis function method and the Brueckner-Hartree-Fock (BHF) approach with realistic

*dongjm07@impcas.ac.cn

nucleon-nucleon interactions [20–23]. In the present work, within the AK framework, we calculate the transport coefficients by adopting the Brueckner theory with the inclusion of the effect of Fermi surface depletion. The bulk viscosity is expected to become the dominant dissipation mechanism for newborn NSs with rather high temperatures ($T > 10^{10}$ K), and we do not consider this situation here.

It is well-known that, the momentum distribution for a perfect Fermi gas follows a right-angle distribution at zero-temperature, namely the well-known Fermi-Dirac distribution. Yet, owing to the short-range repulsive core and tensor interaction (collectively referred to as short-range correlation in some references), the system deviates from the typical profile of an ideal degenerate Fermi gas featured by a high-momentum tail [24–27], and as a result a Fermi surface depletion may appear. The Z-factor measures such a Fermi surface depletion. The correlation between nucleons or its induced Z-factor has far-reaching impact on many issues such as nuclear structure [28, 29], superfluidity of dense nuclear matter [30–32], NS cooling [31] and the European Muon Collaboration effect [33, 34], highlighting its fundamental importance in nuclear physics and NS physics. For instance, Dong et al. have shown that the superfluid gap of β -stable neutron star matter is strongly quenched by the Z factor within the generalized BCS theory [30, 31]. The neutrino emissivity for NS cooling due to direct Urca, modified Urca processes are also reduced by the Z-factor, and therefore the cooling rates of young NSs are considerably slowed [31].

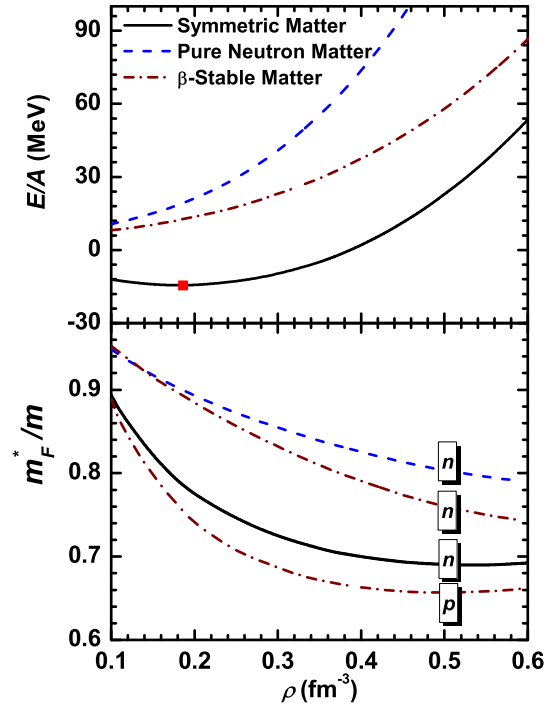


FIG. 1: (a) Energy per particle in symmetric matter, pure neutron matter, and β -stable matter as a function of nucleonic density from the BHF approach. The square shows the position of calculated saturation point. (b) Density-dependent effective mass at Fermi surfaces for three different nuclear matter configurations.

In this work, the roles of the Z-factor in the thermal conductivity and shear viscosity are clarified based on the AK formalism. The neutron triplet superfluidity in NS core quenched by the Z-factor effect is introduced to examine its effects on the viscosity of β -stable NS matter. Then we calculate the shear viscosity timescale and gravitation-wave-driven r -mode growth timescale of canonical NSs to explore whether the shear viscosity is sufficiently strong to damp the r -mode instability. The required in-medium cross sections and nucleon effective masses to calculate transport coefficients, and the Z-factor at the Fermi surface, together with the EOS to establish the NS structure, are all obtained in an unified framework, i.e., the Brueckner theory with AV18 two-body interaction plus a microscopic three-body force [35, 36]. We should stress here that in the calculation the exact treatment of total momentum is adopted to obtain more reliable results [37].

The Z-factor that measures the effect of Fermi surface depletion is given by

$$Z(k) = \left[1 - \frac{\partial \Sigma(k, \omega)}{\partial \omega} \right]_{\omega=\varepsilon(k)}^{-1} \quad (1)$$

with the single-particle energy $\varepsilon(k)$. Where $\Sigma(k, \omega)$ is the self-energy versus momentum k and energy ω . The Z factor at the Fermi surface, labeled Z_F ($0 < Z_F < 1$), is equal to the discontinuity of the occupation number at the Fermi surface, according to the Migdal-Luttinger theorem [38]. Once the nucleon-nucleon correlation is included, the nucleon momentum distribution is given as

$$n(k) = \int \frac{d\omega}{2\pi} S(k, \omega) n^0(\omega) \quad (2)$$

at finite temperature T [39], where ω is the energy. $n^0(\omega) = 1/[1 + \exp(\frac{\omega - \mu}{k_B T})]$ is the well-known Fermi-Dirac distribution function under temperature T and chemical potential μ . The spectral function $S(k, \omega)$ can be expressed as [35]

$$S(k, \omega) \approx Z_F \delta(\omega - \varepsilon(k_F)), k \approx k_F, \quad (3)$$

when momentum k is extremely close to the Fermi momentum k_F . Consequently, the momentum distribution near the Fermi surface is approximated by [31]

$$n(x) \approx Z_F n^0(x), k \approx k_F, \quad (4)$$

with $x = (\varepsilon(k) - \mu)/(k_B T)$. Hereafter we take x as variable in the Fermi-Dirac distribution for convenience. We stress that this approximation is only valid when k is extremely close to the Fermi surface. The nucleon-nucleon correlation quenches the occupation probability by a factor Z_F at Fermi surface k_F , and thus it hinders particle transitions around the Fermi surface.

To embody the effects of nucleonic Fermi surface depletion in the calculation of the kinetic coefficients, we extend the Landau kinetic equation by including the Z-factor in the collision integral. In the AK framework, at temperature T , the collision integral without the Z-factor effect takes the form of [40]

$$\begin{aligned} I_{1i}^0 = & -\frac{m_i^* k_B^2 T^2}{8\pi^4 \hbar^6} \int \int dx_2 dx_3 n^0(x_1) n^0(x_2) [1 - n^0(x_3)] \\ & \times [1 - n^0(x_1 + x_2 - x_3)] \sum_j m_j^{*2} \int \int \frac{d\Omega}{4\pi} \frac{d\phi_2}{2\pi} \\ & \times \frac{W_{ij}(\theta, \phi) \beta_{ij}}{1 + \delta_{ij}} [\psi(\mathbf{p}_1) + \psi(\mathbf{p}_2) - \psi(\mathbf{p}_3) - \psi(\mathbf{p}_4)], \end{aligned} \quad (5)$$

where m^* is the effective mass of nucleon i or j . And the small quantities $\psi(\mathbf{p})$ measures the departure from equilibrium state. Here the nucleon-nucleon scattering is limited to the Fermi surface. For convenience, one can assume 1 and 3 (2 and 4) are the same component, i.e., $|\mathbf{p}_1| = |\mathbf{p}_3| = p_i$ ($|\mathbf{p}_2| = |\mathbf{p}_4| = p_j$). And the transition probability W_{ij} from two quasiparticle state $|\mathbf{p}_1, \mathbf{p}_2\rangle$ to state $|\mathbf{p}_3, \mathbf{p}_4\rangle$, depends only on θ and ϕ ($d\Omega = \sin\theta d\theta d\phi$), where θ is the angle between \mathbf{p}_1 and \mathbf{p}_2 , and ϕ is the angle between the \mathbf{p}_1 - \mathbf{p}_2 plane and \mathbf{p}_3 - \mathbf{p}_4 plane. $\beta_{ij} = p_j/(p_i^2 + p_j^2 + 2p_i p_j \cos\theta)^{1/2}$ reduces to $[2\cos(\theta/2)]^{-1}$ for $i = j$. ϕ_2 is the azimuthal angle of \mathbf{p}_2 with respect to \mathbf{p}_1 . The factor $(1 + \delta_{ij})^{-1}$ takes into account double counting of the final states in the case of like particles.

Due to the temperature T we discussed is several orders of magnitude lower than the nucleonic Fermi temperatures (the nucleons are strong degenerate), the main contribution to the above integral comes from the very narrow regions of momentum space near the corresponding Fermi surfaces k_F , just as the calculation of neutrino emissivity in Ref. [41]. If the Z-factor effect is included, in the above collision integral, $1 - n^0(x)$ (and $n^0(x)$) representing the unoccupied (and occupied) state due to the temperature, should be replaced by $n(x)|_{T=0} - n(x) = Z_F[1 - n^0(x)]$ (and $Z_F n^0(x)$) when the Z-factor effect is included. The collision integral is just attribute to thermal excitations of particles located in a very narrow region of $\sim k_B T$ close to their Fermi surfaces, and the state with $|\varepsilon(k) - \varepsilon(k_F)| \gg k_B T$ plays no role for the collision integral because the thermal energy $k_B T$ is too low to excite those states. Therefore, the high momentum tail makes no contribution to the collision integral, just as the

influence of the Fermi surface depletion on neutrino emissivity processes discussed in detail in Ref. [31]. Consequently, the collision integral turns into

$$\begin{aligned}
I_{1i} = & - \sum_j \frac{Z_{Fi}^2 Z_{Fj}^2 m_i^* m_j^* k_B^2 T^2}{8\pi^4 \hbar^6} \int \int dx_2 dx_3 n^0(x_1) n^0(x_2) \\
& \times [1 - n^0(x_3)] [1 - n^0(x_1 + x_2 - x_3)] \int \int \frac{d\Omega}{4\pi} \frac{d\phi_2}{2\pi} \\
& \times \frac{W_{ij} \beta_{ij}}{1 + \delta_{ij}} [\psi(\mathbf{p}_1) + \psi(\mathbf{p}_2) - \psi(\mathbf{p}_3) - \psi(\mathbf{p}_4)].
\end{aligned} \tag{6}$$

Moreover, the driving term of the Landau kinetic equation, which is proportional to $\frac{\partial n}{\partial x}$ at equilibrium state, provides a Z_F as well. Therefore, one can include the Z -factor effect in the calculation of the transport coefficients by adopting Z_F both in the collision integral and the driving term by following the derivations in Ref. [40]. For example, the collision integral reduces to a simple formula of $I_{1i} = Z_F^4 I_{1i}^0$ for pure neutron matter. One should note that the momentum (energy) flux corresponding to the shear viscosity (thermal conductivity) also includes $\frac{\partial n}{\partial x}$. Consequently, the shear viscosity (thermal conductivity) is given by $\eta = \eta^0/Z_F^2$ ($\kappa = \kappa^0/Z_F^2$) for pure neutron matter, where η^0 (κ^0) is the corresponding transport coefficient without the inclusion of the Z -factor effect.

Within the BHF approach, the EOSs of symmetric nuclear matter ($\beta = 0$), pure neutron matter ($\beta = 1$), and β -stable matter, where $\beta = (\rho_n - \rho_p)/(\rho_n + \rho_p)$ denotes the isospin asymmetry with the neutron (proton) number densities ρ_n (ρ_p), are displayed in Fig. 1(a). The solid square shows the calculated saturation point of symmetric matter which is marginally in agreement with the empirical value due to the introducing of three-body force. The proton fraction in β -stable matter is determined by the density-dependent symmetry energy, i.e., the isospin-dependent part of the EOS. The EOSs for pure neutron matter and β -stable matter show a distinct difference that becomes more and more visible at high densities, indicating the non-negligible proton fraction in NS matter. The NS interior is assumed to be composed of nucleons, electrons and possible muons. With the conditions of electric neutrality and β -equilibrium, the fractions of leptons (electrons and muons as degenerate ideal gas) and their contributions to the energy density $\varepsilon(\rho)$ and pressure $p(\rho)$ can be determined uniquely. With the obtained $\varepsilon(\rho)$ and $p(\rho)$ of the core matter and the EOS from Baym, Pethick, and Sutherland (BPS) [42] for crust matter as inputs, the stellar structure, e.g., the density profile $\rho(r)$ of a static and spherically symmetric NS, is achieved by solving the Tolman-Oppenheimer-Volkov (TOV) equation. The established stellar structure is essential for the final estimation of the shear viscosity timescale and r -mode growth time scale of NSs.

The nucleonic effective mass m^* is defined from the single-particle energy $\varepsilon(p)$ by the relation $m^* = k_F (\partial \varepsilon(k)/\partial k)^{-1}|_{k=k_F}$. It reduces the density of states at the Fermi surface with respect to non-interacting Fermi gas since it is usually smaller than the free mass. As Ref. [23, 43], the rearrangement contribution of three-body force is not included here. The calculated effective mass with the BHF approximation are presented in Fig. 1(b). The neutron effective mass of pure neutron matter is not much different from that of β -stable matter, but is distinctly larger than that of symmetric matter at the same density.

We calculate the in-medium differential sections within the BHF method for symmetric matter, pure neutron matter and β -stable matter, taking the neutron-neutron scattering at density of $\rho = 0.34 \text{ fm}^{-3}$ (twice the saturation density) as an example, as shown in Fig. 2. The free-space cross section is also shown for comparison. The in-medium effect leads to a noticeable suppression of the cross sections, as other calculations within microscopic nuclear many-body approaches, suggesting the important role of the medium effect. Our calculated differential cross sections as functions of center-of-mass scattering angle (and also the total cross sections versus center-of-mass energy $E_{c.m.}$) have the same shape as that in Ref. [23] for density $\rho = 0.35 \text{ fm}^{-3}$, although different three-body forces are used. We would like to stress that, the inclusion of the three-body force increases the cross section at high $E_{c.m.}$, which is in agreement with the conclusion of Ref. [23], but disagrees with the results in Ref. [22, 44].

Figure 3 exhibits the calculated Z_F at Fermi surfaces for three different nuclear matter configurations by employing the Brueckner theory where the self-energy is expanded to the 2nd-order, i.e., $\Sigma = \Sigma_1 + \Sigma_2$. The momentum distribution featured by a high momentum tail and vacant position below the Fermi surface, is illustrated in the inset. The behavior of Z_F for symmetric matter is consistent with the result in Refs. [31, 45]. The Z -factor is caused by the short-range repulsion core and tensor force. The tensor force is dominant at low densities while the short-range repulsion is dominant at high densities. The nonmonotonic

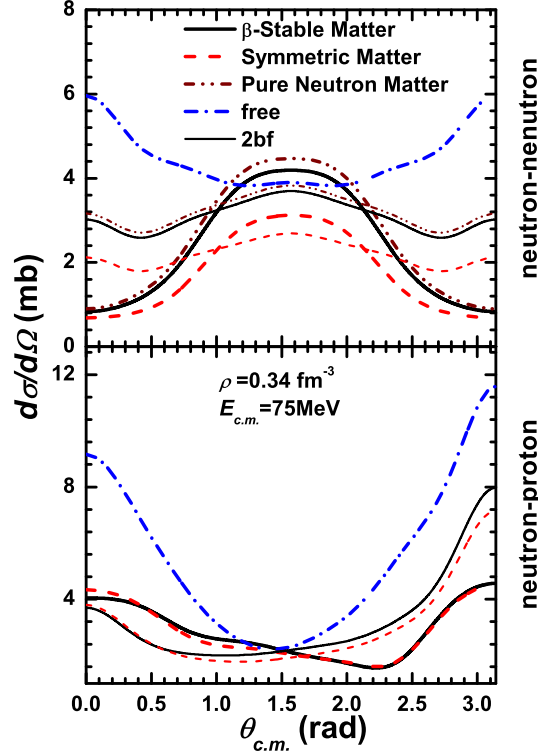


FIG. 2: (a) Differential cross sections of neutron-neutron scattering in symmetric matter, pure neutron matter, and β -stable matter, taking $\rho = 0.34 \text{ fm}^{-3}$ and center-of-mass energy $E_{c.m.} = 75 \text{ MeV}$ as an example. (b) The corresponding total cross sections versus $E_{c.m.}$.

behavior of Z_F for symmetric matter and β -stable matter displayed in Fig. 3 is exactly the results of competition between these two effects, and the Z_F is small both at very low and very high densities. On the other hand, the Z_F exhibits a strong isospin dependence. At a given total nucleon density, the Z_F of symmetric matter is smaller obviously than that of pure neutron matter, that is, the correlation in the former is stronger than that in the later, because the 3SD_1 tensor interaction component between neutrons and protons is quite strong in symmetric matter but is completely absent in pure neutron matter. Namely the pure neutron matter is much closer to the ideal degenerate Fermi gas, as pointed out in Ref. [29]. The results displayed in Fig. 3 will be applied in the following calculations of transport coefficients.

When combining all the results that have been discussed above, we can now compute the density-dependent shear viscosity under various temperatures stemming from nucleon-nucleon collisions. The phase space is quenched in Eq. (2) because of the depletion of Fermi surface, and therefore the thermal conductivity κ and shear viscosity η are increased. The calculated temperature-independent combinations κT and ηT^2 versus density are plotted in Fig. 4, respectively, without and with the inclusion of the Z-factor effect. The lepton (electron and muon) shear viscosity $\eta_{e\mu}$ and thermal conductivity $\kappa_{e\mu}$ mediated by collisions of leptons with charged particles in electrically neutral NS matter, are taken from Ref. [46]. Since the nucleon shear viscosity η_N is mediated by nucleon-nucleon collisions via strong nuclear force, the η_N and $\eta_{e\mu}$ can be treated independently. Yet, the $\eta_{e\mu}$ ($\kappa_{e\mu}$) has different temperature-dependent behavior as η_N (κ_N). So here we show three cases: $T = 10^7$, 10^8 , and 10^9 K . The relation between η_N and $\eta_{e\mu}$ is temperature dependent, that is, η_N becomes more and more important as temperature decreases. The proton contribution to the shear viscosity can be neglected safely since the proton contribution is just 15% even at high density of $\rho = 0.6 \text{ fm}^{-3}$.

The Z-factor effect enhances the nucleonic κ and η for the three nuclear matter configurations, in particular at high densities. For example, at the density of $\rho = 0.6 \text{ fm}^{-3}$, the κ_N and η_N can be enhanced by about three to four times by the Z-factor effect. The nucleonic thermal conductivity is much larger than the lepton ones for all densities of NS matter and temperatures of interest. Yet, the situation is different for shear viscosity. Without the Z-factor effect ($Z = 1$), the primary contribution to

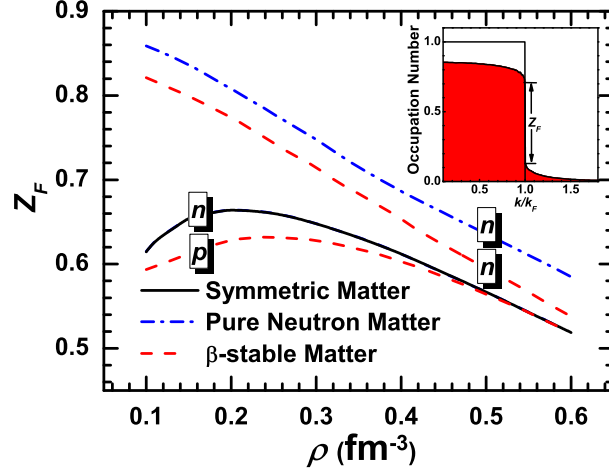


FIG. 3: Density-dependent Z -factor at Fermi surfaces in symmetric matter, pure neutron matter, and β -stable matter. The inset presents a schematic illustration of the Fermi surface depletion induced by the nucleon-nucleon correlation.

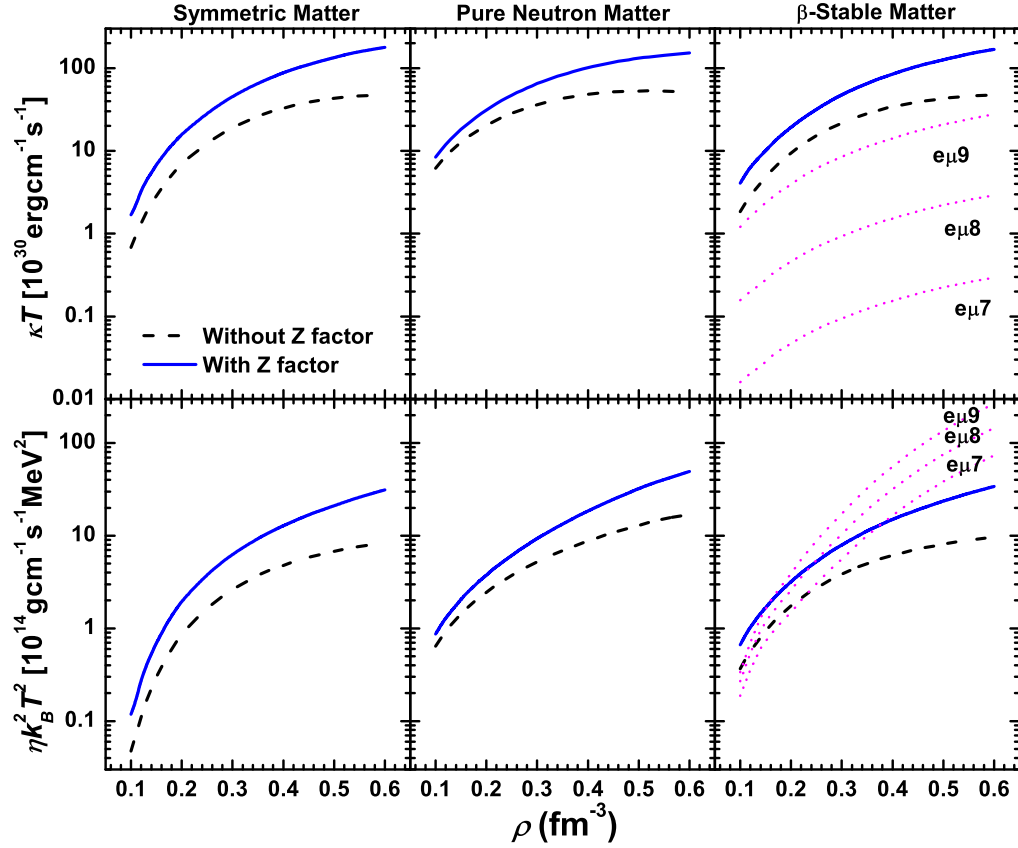


FIG. 4: Thermal conductivity κ (upper panel) and shear viscosity η (lower panel) of nucleons and leptons as a function of density in symmetric matter, pure neutron matter, and β -stable matter. The nucleonic κ_N and η_N are calculated with the help of BHF approach without and with the inclusion of Z -factors.

the shear viscosity $\eta = \eta_N + \eta_{e\mu}$ comes from the lepton scattering which is just exceeds by nucleon scattering at low densities, in agreement with the conclusion of Ref. [23]. Once the Z-factor is taken into account, the η_N and $\eta_{e\mu}$ become comparable at intermediate densities, and the η_N is about four times larger than $\eta_{e\mu}$ at crust-core transition density $\rho \approx 0.08 \text{ fm}^{-3}$.

It is widely believed that superfluidity plays a crucial role in NS dynamics, such as NS cooling and the observed pulsar glitch. It draw wide attention in communities of nuclear physics and NS physics in particular after the rapid cooling of the NS in Cassiopeia A was observed. The strong nuclear force provides several attractive channels between nucleons in which superfluidity is possible [47–49]. The neutrons dripped out from the neutron-rich nuclei in NS inner crust, are expected to be paired in a 1S_0 singlet state with energy gap of $\sim 1.5 \text{ MeV}$ [50]. The proton gas is so dilute that the proton 1S_0 superconductivity (superfluidity of charged particles) may survive until deep inside the star but the neutron 1S_0 superfluidity vanishes because the nuclear interaction in the 1S_0 channel becomes repulsive at short distances for high neutron density. Nevertheless, at high density, neutron-neutron coupling in the 3PF_2 anisotropic pairing state could appear owing to the attractive component of the nuclear interaction in this coupling channel. The coupling between the 3P_2 and 3F_2 states is attributed to tensor force. This neutron 3PF_2 superfluidity is of great interest because it was employed to explain the rapid cooling of the NS in Cassiopeia A [3]. However, the superfluidity may reduced significantly by the nucleon-nucleon correlation [30, 31, 51]. By performing fittings with several parameters, the density-dependent gap for the neutron 3PF_2 superfluidity of β -stable matter is given by [52]

$$\Delta_n(\rho) = (0.943\rho - 0.050) \exp \left[- \left(\frac{\rho}{0.177} \right)^{1.665} \right], \quad (7)$$

with a peak value of about 0.04 MeV at $\rho = 0.17 \text{ fm}^{-3}$. The proton 1S_0 superfluid gap exists in a rather narrow region and is much smaller than the neutron 3PF_2 superfluid gap as stressed in [52]. In addition, the proton fraction is much smaller than the neutron one for β -stable NS matter. Therefore, we do not consider it in the present work. Here we only focus on the effects of neutron triplet superfluidity on shear viscosity. As mentioned in Ref. [53], we introduce a suppression factor to estimate the nucleon shear viscosity via $\eta_N^{(\text{SF})} \approx R_n \eta_N$, where R_n is written as [53]

$$R_n \simeq \left[0.9543 + \sqrt{0.04569^2 + (0.6971y)^2} \right]^3 \cdot \exp \left[0.1148 - \sqrt{0.1148^2 + 4y^2} \right] \quad (8)$$

with $y = \Delta(T)/T$. $\Delta(T)$ is the temperature-dependent energy gap, and the critical temperature is $T_c = 0.57\Delta(T=0)$. The η_N due to neutron-neutron scattering drops exponentially because of sharp decrease of the number of momentum carriers near the Fermi surface.

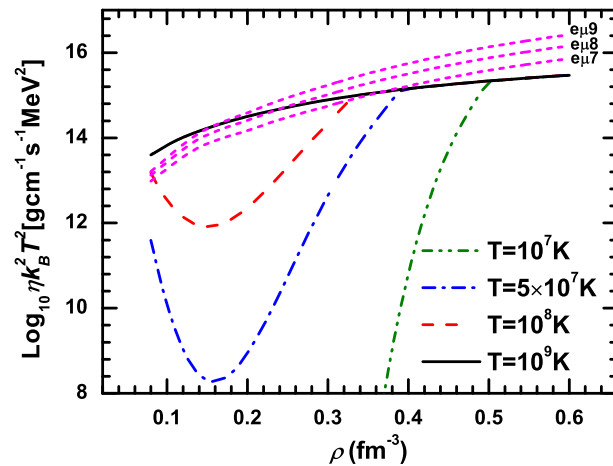


FIG. 5: Shear viscosity stemming from nucleon-nucleon scattering as a function of density in β -stable matter with the inclusion of neutron triplet superfluidity.

The ηT^2 of each component as a function of density under different temperatures T in the presence of neutron 3PF_2 superfluidity are displayed in Fig. 5. If the core temperatures of NSs are higher than $\sim 2 \times 10^8$ K, the neutron 3PF_2 superfluidity disappears. The neutrons in stellar core becomes superfluid as soon as the NS cools below the critical temperatures, and accordingly the neutron-neutron scattering is strongly depressed and the main contribution to the shear viscosity comes from electron scattering processes. As a result, the Z-factor-quenched superfluid effect plays an opposite role compared with the Z-factor effect itself, and intriguingly it can be much more significant. For instance, at the temperature $T = 5 \times 10^7$ K, the nucleon shear viscosity η_N is reduced by about six orders of magnitude at $\rho = 0.17 \text{ fm}^{-3}$, and this suppression is stronger at lower temperatures. It was concluded in other references such as [18] that, at low temperatures $T < 10^7$ K, the contribution to the shear viscosity from the neutron scattering is more important than the lepton scattering. However, the $\eta_{e\mu}$ is still larger than η_N in the presence of such neutron triplet superfluidity. For example, at temperature $T = 10^7$ K, the η_N of the nucleon scattering can be neglected at density $\rho < 0.5 \text{ fm}^{-3}$ in superfluid matter.

TABLE I: The calculated shear viscosity time scale τ_η , compared with gravitation-radiation-driven r -mode time scale $\tau_{\text{GW}} = 196$ s for canonical neutron stars rotating at 716 Hz. The results with and without the neutron triplet superfluidity (SF) are listed, and the weights of the nucleon contribution are present in the brackets.

Temperature (K)	$\tau_\eta^{\text{nSF}}(\text{s})$	$\tau_\eta^{\text{SF}}(\text{s})$
10^6	402 (66%)	1200 (0%)
10^7	2.99×10^4 (50%)	4.38×10^4 (9%)
10^8	2.05×10^6 (34%)	2.26×10^6 (27%)
10^9	1.38×10^8 (23%)	1.07×10^8 (23%)

After the stellar structure is established by solving the TOV equation with the BHF EOS as an input, the time scales of shear viscosity and of gravitation-radiation-driven growth of r -mode for $1.4M_\odot$ canonical NSs are calculated. The overall time scale is $1/\tau = -1/\tau_{\text{GW}} + 1/\tau_\eta$, and if angular-velocity-dependent τ_{GW} is smaller than temperature-dependent τ_η , the r -mode amplitude will exponentially grow, resulting in r -mode instability. The equation of $1/\tau = 0$ determines the critical frequency in frequency-temperature space, above which is the usually referred to as the r -mode instability window [54, 55].

Table I lists the calculated shear viscosity τ_η and r -mode growth time scale τ_{GW} for canonical NSs. In non-superfluid NSs, the nucleon-nucleon scattering is indeed the dominant dissipation mechanism at low temperatures. If the superfluid effect is included, the situation is completely opposite. The η_N becomes less and less important and even negligible as temperature decreases. The τ_η is enlarged because of the superfluid effect, indicating weaker shear viscosity damping. It is generally believed that the r -mode instability limits the rotating angular velocity of accretion millisecond pulsars. At present, the fastest spinning pulsar is PSR J1748-2446ad spinning at 716 Hz [56], and its corresponding r -mode growth time scale τ_{GW} is 196 s if $M_{\text{TOV}} = 1.4M_\odot$ is assumed. At low temperatures $T = 10^6$ K, the shear viscosity τ_η is 402 Hz for nonsuperfluid NS core matter which is comparable with the τ_{GW} , and the weight of nucleonic contribution is as large as 66%. However, if the superfluidity is taken into account, the nucleon-nucleon scattering does not contribute to the τ_η at such low temperature, and the τ_η is much larger than the τ_{GW} and hence the shear viscosity is not much help to damp the r -mode instability. Some authors proposed that the viscous dissipation at the viscous boundary layer of perfectly rigid crust and fluid core is the primary damping mechanism. However, it is questioned if the core-crust boundary is defined by a continuous transition from non-uniform matter to uniform matter through "nuclear pasta" phases [57] and consequently the viscous boundary layer is smeared out [58].

In order to more clearly reveal the roles of the Z-factor and superfluid effects on the r -mode instability, the calculated r -mode instability critical curves are presented in Fig. 6. The Z-factor effect is conducive to damping the gravitational-wave-driven r -mode growth of NSs, in particular at low temperatures. However, the neutron triplet superfluidity plays an opposite role and is more significant. At temperatures higher than $\sim 10^8$ K, both of the two effects are weak, which is because the neutron-neutron scattering contributes secondary to shear viscosity and the superfluidity is almost vanishes at such temperatures. The core temperature of NSs in low mass X-ray binaries are estimated to be $(1 \sim 5) \times 10^8$ K [59] and $10^7 \sim 10^8$ K if the direct Urca process opens [52], therefore the shear viscosity cannot be expected to stabilize NSs against r -mode oscillations in practical situation. Additional damping mechanisms perhaps is required.

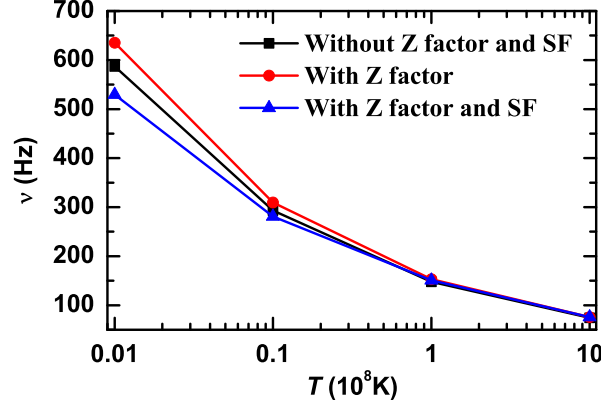


FIG. 6: The calculated r -mode instability critical curves without the superfluidity (SF) and Z-factor, with Z-factor only, with both the Z-factor and neutron triplet superfluidity, are shown for comparison.

In summary, the Z-factor effects on the thermal conductivity and shear viscosity have been calculated based on the AK framework, where the Z-factor at Fermi surfaces (Z_F), the in-medium cross sections, nucleon effective masses, and the EOS of NS matter, are calculated by using the Brueckner theory with the two-body AV18 interaction plus microscopic three-body force. The nucleon-nucleon correlations, induced by the effects of short-range repulsion and tensor component of nuclear force, gives rise to the Fermi surface depletion, i.e., the Z-factor effect. The calculated Z_F of neutrons and protons at Fermi surfaces presents a strong isospin dependence due to the strong neutron-proton 3SD_1 tensor interaction. The two transport coefficients are enlarged by several times for symmetric matter, pure neutron matter and β -stable matter. The nucleonic thermal conductivity κ_N is much more important than lepton ones for different densities and temperatures that we considered here, whether or not this Z-factor effect is included. As temperature decreases, the nucleon shear viscosity η_N becomes more and more important with respect to the lepton contribution $\eta_{e\mu}$. If we take into account the Z-factor effect, the η_N may become comparable with $\eta_{e\mu}$ at intermediate densities, and larger than $\eta_{e\mu}$ at low densities. As concluded in the previous works [30, 31], the Z-factor effect suppresses the proton 1S_0 and neutron 3PF_2 superfluidity strongly, and the proton 1S_0 superfluidity almost vanishes. Contrary to the role of Z-factor itself, neutron superfluidity is able to reduce the shear viscosity significantly (by several orders of magnitude) when the temperature drops below the critical temperature. As a result, the contribution to the shear viscosity from the lepton scattering is still more important than that from the nucleon scattering at low temperature for the densities of interest in superfluid matter. Finally, the shear viscosity time scales τ_η along with the time scales τ_{GW} of r -mode growth due to the emission of gravitational waves for canonical NSs are calculated. At low temperatures, the nucleon-nucleon scattering indeed contributes mainly to the shear viscosity time scale τ_η . However, if the Z-factor-quenched superfluidity is present, it is less important and even negligible. In a word, the appearance of superfluidity is not favorable to damping the r -mode instability of NSs. The calculated τ_η is much larger than the τ_{GW} and hence the shear viscosity is not able to damp the r -mode instability even for very cold NSs with core temperature of 10^6 K. The present work stretches our understanding of the r -mode instability of pulsar physics.

This work was supported by the National Natural Science Foundation of China (Grants No. 11775276, 11975282), the Strategic Priority Research Program of Chinese Academy of Sciences (Grant No. XDB34000000), the Youth Innovation Promotion Association of Chinese Academy of Sciences (Grant No. Y201871), the Continuous Basic Scientific Research Project (Grant No. WDJC-2019-13), the Leading Innovation Project (Grant No. LC 192209000701), and the Continuous Basic Scientific

-
- [1] P. Haensel, A. Y. Potekhin, D. G. Yakovlev, *Neutron Stars I*, (Springer, 2006).
 - [2] P. S. Shternin, et al., Mon. Not. Roy. Astron. Soc. 412 (2011) L108.
 - [3] D. Page, M. Prakash, J. M. Lattimer, A. W. Steiner, Phys. Rev. Lett. 106 (2011) 081101.
 - [4] A. Sedrakian, Astron. Astrophys. 555 (2013) L10.
 - [5] D. Blaschke, H. Grigorian, D. N. Voskresensky, F. Weber, Phys. Rev. C 85 (2012) 022802(R).
 - [6] W. G. Newton, K. Murphy, J. Hooker, B.-A. Li, Astrophys. J. 779 (2013) L4.
 - [7] A. Bonanno, M. Baldo, G. F. Burgio, V. Urpin, Astron. Astrophys. 561 (2014) L5.
 - [8] W. C. G. Ho, K. G. Elshamouty, C. O. Heinke, A. Y. Potekhin, Phys. Rev. C 91 (2015) 015806.
 - [9] S. Chandrasekhar, Astrophys. J. 161 (1970) 561.
 - [10] J. L. Friedmann, B. F. Schutz, Astrophys. J. 221 (1978) 937; 222 (1978) 281.
 - [11] L. Lindblom, B. J. Owen, S. M. Morsink, Phys. Rev. Lett. 80 (1998) 4843.
 - [12] L. Bildsten, Astrophys. J. 501 (1998) L89.
 - [13] N. Andersson, K. D. Kokkotas, N. Stergioulas, Astrophys. J. 516 (1999) 307.
 - [14] D. Page, U. Geppert, F. Weber, Nucl. Phys. A 777 (2006) 497.
 - [15] D. G. Yakovlev, C. J. Pethick, Annu. Rev. Astron. Astrophys. 42 (2004) 169.
 - [16] E. Flowers, N. Itoh, Astrophys. J. 230 (1979) 847.
 - [17] C. Cutler, L. Lindblom, Astrophys. J. 314 (1987) 234.
 - [18] I. Vidana, Phys. Rev. C 85 (2012) 045808.
 - [19] A. A. Abrikosov, I. M. Khalatnikov, Sov. Phys. JETP 5 (1957) 887; Rep. Prog. Phys. 22 (1959) 329.
 - [20] O. Benhar, M. Valli, Phys. Rev. Lett. 99 (2007) 232501.
 - [21] O. Benhar, A. Polls, M. Valli, I. Vidana, Phys. Rev. C 81 (2010) 024305.
 - [22] H. F. Zhang, U. Lombardo, W. Zuo, Phys. Rev. C 82 (2010) 015805.
 - [23] P. S. Shternin, M. Baldo, P. Haensel, Phys. Rev. C 88 (2013) 065803.
 - [24] J. P. Jeukenne, A. Lejeune, C. Mahaux, Phys. Rep. 25 (1976) 83.
 - [25] A. Ramos, A. Polls, W. H. Dickhoff, Nucl. Phys. A 503 (1989) 1.
 - [26] B. E. Vonderfecht, W. H. Dickhoff, A. Polls, A. Ramos, Nucl. Phys. A 555 (1993) 1.
 - [27] P. Yin, J. Dong, W. Zuo, Chin. Phys. C 41 (2017) 114102.
 - [28] R. Subedi, et al., Science 320 (2008) 1476.
 - [29] O. Hen, et al., Science 346 (2014) 614.
 - [30] J. M. Dong, U. Lombardo, W. Zuo, Phys. Rev. C 87 (2013) 062801(R).
 - [31] J. M. Dong, U. Lombardo, H. F. Zhang, W. Zuo, Astrophys. J. 817 (2016) 6.
 - [32] Bao-An Li, Bao-Jun Cai, Lie-Wen Chen, Jun Xu, Prog. Part. Nucl. Phys. 99 (2018) 29.
 - [33] O. Hen, G. A. Miller, E. Piasetzky, L. B. Weinstein, Rev. Mod. Phys. 89 (2017) 045002.
 - [34] The CLAS Collaboration, Nature 560 (2018) 617.
 - [35] M. Baldo, I. Bombaci, G. Giansiracusa, U. Lombardo, C. Mahaux, and R. Sartor, Phys. Rev. C 41 (1990) 1748 ; Nucl. Phys. A 545 (1992) 741.
 - [36] W. Zuo, I. Bombaci, U. Lombardo, Phys. Rev. C 60 (1999) 024605.
 - [37] X. L. Shang, J. M. Dong, W. Zuo, P. Yin, U. Lombardo, (unpublished).
 - [38] A. B. Migdal, Sov. Phys. JETP 5 (1957) 333; J. M. Luttinger, Phys. Rev. 119 (1960) 1153.
 - [39] L. P. Kadanoff, G. Baym, *Quantum Statistical Mechanics*, (New York, 1962).
 - [40] R. H. Anderson, C. J. Pethick, and K. F. Quader, Phys. Rev. B 35 (4) (1987) 1620.
 - [41] D. G. Yakovlev, A. D. Kaminker, O. Y. Gnedin, P. Haensel, Phys. Rep. 354 (2001) 1.
 - [42] G. Baym, C. J. Pethick, P. Sutherland, Astrophys. J. 170 (1971) 299; G. Baym, H. A. Bethe, C. J. Pethick, Nucl. Phys. A175 (1971) 225.
 - [43] X. L. Shang, A. Li, Z. Q. Miao, G. F. Burgio, H. J. Schulze, Phys. Rev. C 101 (2020) 065801.
 - [44] H. F. Zhang, Z. H. Li, U. Lombardo, P. Y. Luo, F. Sammarruca, and W. Zuo, Phys. Rev. C (2007) 054001.
 - [45] Z. X. Yang, X. L. Shang, G. C. Yong, W. Zuo, Y. Gao, Phys. Rev. C 100 (2019) 054325.
 - [46] P. S. Shternin, D. G. Yakovlev, Phys. Rev. D 78 (2008) 063006.

- [47] D. J. Dean and M. Hjorth-Jensen, *Rev. Mod. Phys.* 75 (2003) 607.
- [48] S. Frauendorf and A. O. Macchiavelli, *Prog. Part. Nucl. Phys.* 78 (2014) 24.
- [49] X. L. Shang, W. Zuo, *Phys. Rev. C* 88 (2013) 025806.
- [50] U. Lombardo, H.-J. Schulze, *Physics of Neutron Star Interiors*, edited by D. Blaschke, N. K. Glendenning, and A. Sedrakian, Lecture Notes in Physics Vol. 578, (Springer-Verlag, Berlin and Heidelberg, 2001), pp. 30–C54.
- [51] X. H. Fan, X. L. Shang, J. M. Dong, W. Zuo, *Phys. Rev. C* 99 (2019) 065804.
- [52] J. M. Dong, (unpublished).
- [53] N. Andersson, G. L. Comer, K. Glampedakis, *Nucl. Phys. A* 763 (2005) 212.
- [54] N. Andersson, K. D. Kokkotas, *Int. J. Mod. Phys. D* 10 (2001) 381.
- [55] B. Haskell, *Int. J. Mod. Phys. E* 24 (2015) 1541007.
- [56] J. W. T. Hessels, et al., *Science* 311 (2006) 1901.
- [57] C. Pethick, A. Y. Potekhin, *Phys. Lett. B* 427 (1998) 7.
- [58] M. Gearheart, W. G. Newton, J. Hooker, B. Li, *Mon. Not. Roy. Astron. Soc.* 418 (2011) 2343.
- [59] W. C. G. Ho, N. Andersson, B. Haskell, *Phys. Rev. Lett.* 107 (2011) 101101.